ANL-77-40

ANL-77-40

SUMMARY AND EVALUATION OF TRANSIENT TEST DATA ON EXTENDED FUEL MOTION RESULTING FROM UNPROTECTED LOSS OF FLOW

by

C. E. Dickerman

BASE TECHNOLOGY

ARGONNE NATIONAL LABORATORY, ARGONNE, ILLINOIS

Prepared for the U. S. ENERGY RESEARCH AND DEVELOPMENT ADMINISTRATION under Contract W-31-109-Eng-38

DISCLAIMER

Printed in the United States of America
Available from
National Technical Information Service
U. S. Department of Commerce
5285 Port Royal Road
Springfield, Virginia 22161
Price: Printed Copy $4.~~00~~ 50; Microfiche $3.00

Distribution Category:
LMFBR Safety (UC-79p)

ANL-77-40

ARGONNE NATIONAL LABORATORY
9700 South Cass Avenue
Argonne, Illinois 60439

SUMMARY AND EVALUATION OF TRANSIENT TEST DATA ON EXTENDED FUEL MOTION RESULTING FROM UNPROTECTED LOSS OF FLOW

by

C. E. Dickerman

Reactor Analysis and Safety Division

June 1977

THIS PAGE

WAS INTENTIONALLY

LEFT BLANK

TABLE OF CONTENTS

LIST OF FIGURES

LIST OF TABLES

SUMMARY AND EVALUATION OF TRANSIENT TEST DATA ON EXTENDED FUEL MOTION RESULTING FROM UNPROTECTED LOSS OF FLOW

by

C. E. Dickerman

ABSTRACT

Experimental data on fuel failure and its consequences are used to provide predictions of the extended fuel motion that would occur after a hypothetical core-disruptive loss-of-flow accident without scram in the Fast Test Reactor. These data indicate the existence of fuel-dispersal mechanisms, slow collapse of fresh fuel, resistance to collapse of irradiated fuel, the absence of accelerated collapse mechanisms (such as cladding-coolant vapor "explosions"), and the fact that real LMFBR conditions inhibit rapid sodium-vaporization events. These data indicate that severely damaged subassemblies will not be coolable in situ by returning sodium after the accident, because of steel and fuel blockages, and suggest that the severely damaged, melted fuel will eventually disperse upward under the influence of vapor generated by decay heating.

I. INTRODUCTION

A. Goal

This status summary documents the application of experimental data to provide predictions of extended fuel motion from the core region resulting from a Fast Test Reactor (FTR) loss-of-flow (LOF) hypothetical core-disruptive accident. This summary will consider the conditions expected to affect significant fuel motion and take into account the need to extrapolate from small-scale tests to full-scale LMFBR geometry. The outline followed is as follows:

1. Extended fuel-cladding motion resulting directly from loss of flow.
   a. Fresh fuel
   b. Irradiated fuel

2. Extended fuel motion resulting directly from a power excursion generated by reactivity insertion produced by fuel slumping caused by loss of flow.

   a. Fresh fuel

      (1) Boundary conditions influencing extended fuel motion.
      (2) Movement of slumped fuel.
      (3) Movement of standing fuel.

   b. Irradiated fuel

      (1) Boundary conditions influencing extended fuel motion.
      (2) Movement of melted fuel.
      (3) Movement of standing fuel.

3. Fuel survival

   a. Loss of flow

   b. Power burst triggered by loss of flow

   c. Survival after power burst

4. Postaccident fuel condition

   a. Reentry fuel-cladding interaction (FCI)

   b. Fuel (cladding) locations and conditions (coolability)

B. Approach

The sequences of events predicted for an LOF hypothetical core-disruptive accident in the FTR will be described using data from applicable transient tests performed before March 1, 1974, principally those TREAT loop experiments with oxide fuel that produced fuel failure[1-3] (see Table I). Some additional tests are also referenced, where necessary, to provide better perspective. The full list of tests covered is given later in Table III. Section II provides the predicted sequences of events in terms of application to a loss-of-flow analysis scenario. Condensed summaries of the actual test results supporting Sec. II appear in Sec. III. For details, consult the references at the end of this report.

Although details of loss-of-flow accident analyses change with such input parameters as core-loading patterns and core-physics data, a general pattern for FTR can be outlined from calculations. FTR core-void coefficients of reactivity are not sufficiently large that core voiding from either boiling or fission-gas release will drive the reactor prompt critical. Coherent fuel slumping in the higher-power subassemblies is the mechanism for reactivity input. If the core power stays relatively constant and fuel maintains its geometry, the time for boiling to be initiated across the entire core is a few seconds.

TABLE I. Summary of TREAT Loop Tests Producing Failure of Oxide Fuel

Test Designation	No. of Fuel Pins	Fuel Burnup, at. %	Fuel Length, in. (cm)	Sample Energy at Failure,[a] J/g	Max Fuel at Solidus at Failure, areal %	Max Bulk Coolant Temp at Time of Failure, °F (°C)	Estimated Energy Conversion to Work, J/g
Unshaped Transients							
E2	1	Fresh	11.6 (29.5)	1800	92	860 (460)	1
	6	Dummies					
H2	1	Fresh	13.5 (34.3)	1190	76	1470 (800)	0.15
E3	3	~6	5.7 (14.5)	855	(0)	1050 (565)	3
E4	1	Fresh	13.5 (34.3)	1420	~100	1730 (944)	0.85
Shaped Transients							
H4	1	4.4	13.5	820	20		
	6	Fresh	13.5	1170	60	1395 (725)	0.2
H5	1	3.5	13.5 (34.3)	755	10	1300 (703)	0.1
	6	Fresh	13.5 (34.3)	1090[b]	55[b]		
E6	1	4.3	13.5 (34.3)	1170	80	1750 (954)	0.2
	6	Fresh	13.5 (34.3)	1380[b]	~100[b]		
E7[c]	7	4.3	13.5 (34.3)	855[b]	15[b]	1270 (687)	0.3
L2	7	Fresh	13.5 (34.3)	[Flattop at sample power of 11 kW/ft (36 kW/m)]			-
L3	7	3.5	13.5 (34.3)	[Flattop at sample power of 9 kW/ft (29.5 kW/m)]			-
L4	7	4.3	13.5 (34.3)	[Flattop at sample power of 10 kW/ft (33 kW/m)]			-
R3	1	Fresh	36 (91.4)	[Flattop at sample power of 10 kW/ft (33 kW/m)]			-
R4	7	Fresh	36 (91.4)	[Flattop at sample power of 10 kW/ft (33 kW/m)]			-
R5	7	Fresh	36 (91.4)	[Flattop at sample power of 10 kW/ft (33 kW/m)][d]			-

[a]Radial average at elevation of region of failure. For shaped transients with well-developed radial temperature profiles, the maximum local enthalpy is much higher. Note next column. Estimate corrected for heat losses during shaped transients.

[b]Highest-energy pin.

[c]No dramatic pressure or flow anomalies; "failure" is associated with beginning of a mild voiding event.

[d]Power terminated at point between cladding melting and fuel melting.

Thus subassembly conditions over the core at the time of an LOF slumping-induced power burst can range from molten-fuel slumping in a voided channel to intact fuel in an unvoided channel. Although the slumping-induced reactivity is not expected to be sufficient to generate a core disassembly, extended fuel motion would result.

Figures 1 and 2 depict the posttest radiographs of the loop test sections from three TREAT LOF and three transient overpower (TOP) tests, respectively. It will be instructive to review these figures with reference to Secs. II and III. In each case, the radiography was performed after loop outfitting (neutron filters, shaping collars, heaters, etc.) had been removed to remove extraneous images. In one case (L2), neutron radiography was not available after this removal operation, and X radiography was performed. For the other five cases, neutron radiography was performed. In these cases, the radiation was

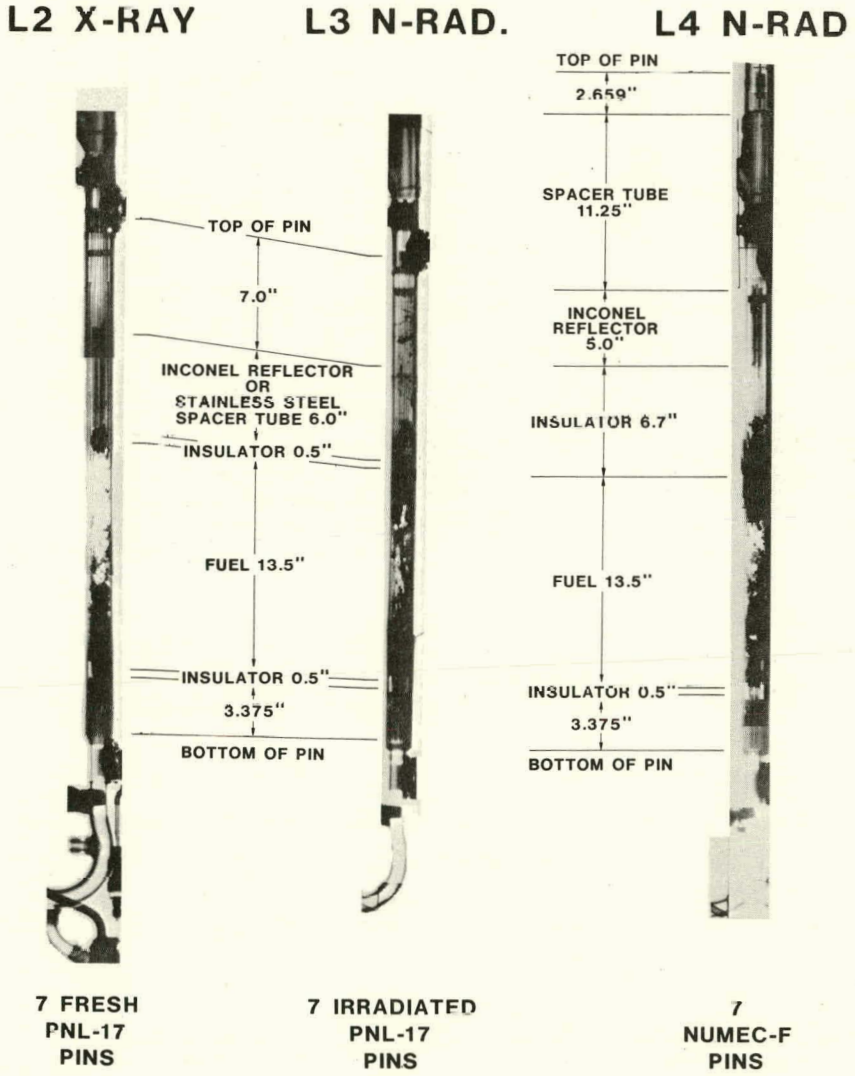

Fig. 1. Posttest Radiographs Showing Fuel Distributions Produced in Three LOF Tests. Conversion factor: 1 in. = 2.54 cm. ANL Neg. No. 900-3329.

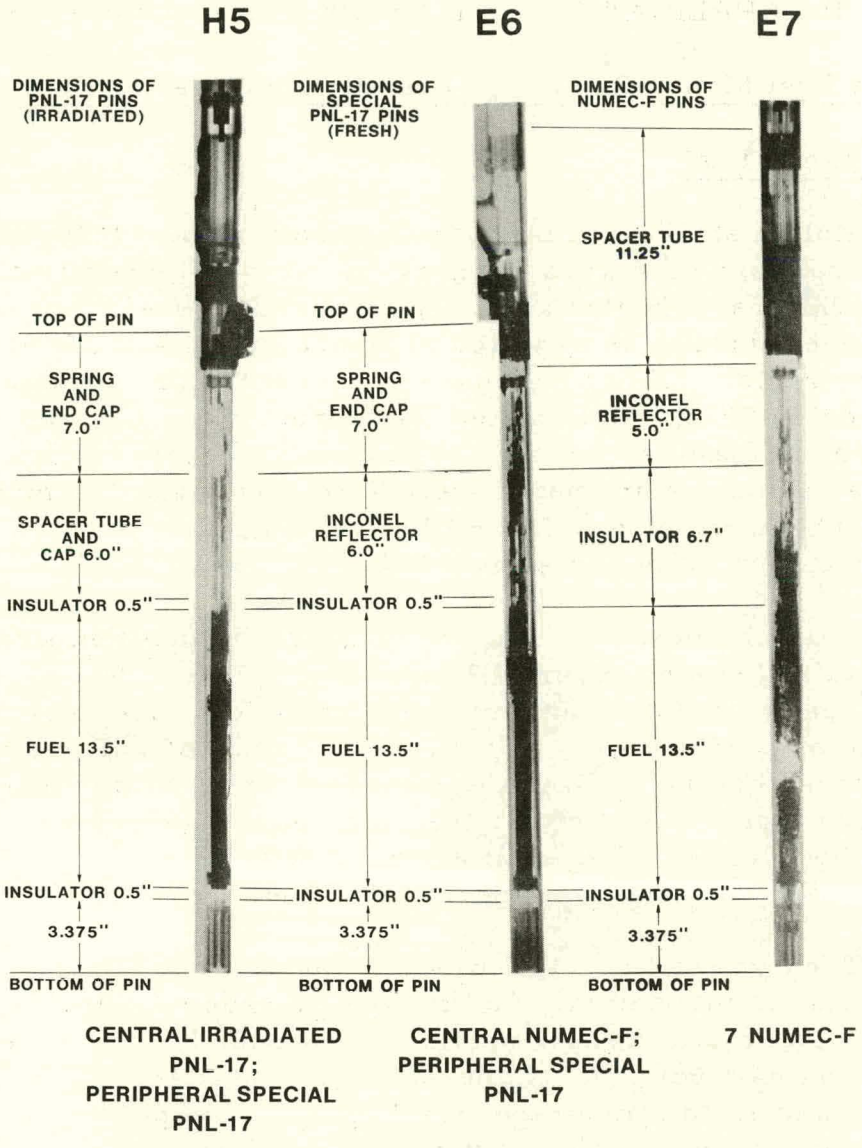

Fig. 2. Posttest Radiographs Showing Fuel Distributions Produced in Three TOP Tests. Conversion factor: 1 in. = 2.54 cm. ANL Neg. No. 900-3773.

preferentially absorbed in enriched oxide. All six images are printed to show absorption: the greater the radiation absorption, the darker the image. The initial locations of pin components are noted for each test section.

None of the tests available for this summary directly simulated a power burst after the "lead subassemblies" had undergone flow coastdown, voiding, and melting of cladding and fuel. However, as apparent from the conditions detailed in the outline, the TOP tests did mock up some key conditions expected to exist at the time of an LOF-induced power burst. Thus, these TOP test data may be applied to descriptions of LOF-induced TOP scenarios if proper account is taken of the differences that exist in the tests. Safety research is showing that the later stages of the accident scenarios and consequences of LOF and TOP accidents in LMFBR's are converging.

II. APPLICATION TO LOSS-OF-FLOW ANALYSES

A. Extended Fuel Motion Resulting Directly from Loss of Flow

1. Fresh Fuel

Molten steel cladding is carried both upward (presumably driven by sodium vapor) and downward (by gravity). A small quantity of molten steel solidifies in the first unheated axial region above the fuel. However, most of the molten-steel cladding is expected to run down and solidify at the bottom of the fuel-stack region. This behavior is consistent with the predictions of the CLAZAS module of SAS. Molten steel is carried upward by sodium vapor; the steel solidifies in the first unheated region and "triggers" a flow blockage, after which an extensive amount of steel flows downward and forms a large, lower plug. The upper plug (a few millimeters high), however, is much thinner than calculated by current models.

After the flow channels are plugged, the fuel temperature continues to rise, and fuel slumping occurs. There is no evidence for the existence of accelerated compaction mechanisms, such as molten-cladding/coolant interactions at the ends of the fuel. In fact, the presence of walls and two-phase fuel should cause the fuel collapse to be significantly slower than free fall. Fuel does not penetrate past either the lower or the upper plug of solidified steel. Postslumping fuel-dispersal events or eructations occur, but do not cause fuel to penetrate the thin, upper, solidified steel plug.

The first fuel eructation is attributed to the vapor pressure of steel constitutents in the interior of a fuel mass with crusted exterior. The solidified steel and fuel block the test-section flow channels at both the top and bottom of the original fuel stack. The effect of the steel plugs is shown in the posttest L2 neutron radiograph (see Fig. 1). This prediction is based on small-scale tests with seven-pin clusters, conducted with experimental conditions designed to simulate coolant-channel and cladding-heating distributions that approximate those typical of the central pins of a large subassembly.

In larger clusters, there may be a difference in cladding motion between the internal channels and the cooler peripheral channels. (No significant difference was seen in the TREAT test remains.) If, in a large cluster, molten cladding is not carried over from hotter internal channels to adjacent peripheral channels, then there might be some survival of pin geometry in peripheral channels beyond the time indicated by this scenario.

2. Irradiated Fuel

A limited amount of molten cladding will move upward and solidify in a thin blockage at the top insulator region--the first unheated region above the fuel. More molten steel will flow downward and solidify at the bottom of

the fuel. These solidified steel regions are also consistent with the prediction of the CLAZAS module of SAS as regards location, but the extents of the blockages produced (a few millimeters high) are much smaller than calculated by current models. No collapse of irradiated fuel occurs; rather, the oxide is expected to move laterally, with some tendency for both steel and fuel material to move outward radially. Consequently, less solidified steel is expected, at least initially, at the bottom of the fuel than for the fresh-fuel case.

No fuel dispersal (gas driven or otherwise) is expected to occur at a time corresponding to that of the first slumping of fresh fuel. However, a fuel dispersal or eructation will occur at conditions corresponding to those of the fresh-fuel eructation. For both fresh and irradiated fuel, the vapor pressure of the steel is the mechanism identified as the source for the eructation. This dispersal pushes some fuel a small distance past the locations of the thin, top solidified-steel "plug"; the original fueled region is not emptied, but most of the fuel is moved upward from the upper two-thirds of the fuel stack.

In addition (note the high-power fuel Test L4), some fuel below the original axial center may be dispersed downward, and the details of the dispersal may generate some net fuel motion toward the center. However, no increase in fuel density beyond the original smeared density is expected on the basis of Test L4. The solidified fuel residue will block the coolant-flow channels at both the top and bottom of the original fuel stack. No fuel-compaction mechanisms can be justified by these experimental data. (See the radiographs of L3 and L4 in Fig. 1.)

B. Extended Fuel Motion Resulting Directly from Power Excursion Produced by Reactivity Feedback Caused by Loss of Flow

1. Fresh Fuel

a. Loss-of-flow-produced Boundary Conditions Influencing Extended Fuel Motion. Test data were examined for LOF-produced conditions that could limit possible subsequent fuel motion. One such phenomenon was found--steel plugs at the ends of the fuel. Steel cladding that melts after coolant voiding solidifies into steel plugs at top and bottom in the first unheated sections. The top plug is expected to be thin, nominally a few millimeters thick. The small size of the experimental test sections did not cause anomalous steel freezing in the tests, because the steel froze to the first unheated material, without evidence of "bridging" from the heat sink of the test-section walls. Steel merely melted at or near the top of the fuel, moved up, and froze.

b. Movement of Slumped Fuel. Fuel will disperse from the slumped condition. However, there is no mechanism for maintaining the initial contact of the dispersed fuel with the upper steel plug. Hence, the initial dispersals are not expected to cause meltthrough of fuel past this plug. (In L2, the timing of the first eructation was consistent with a vapor-driven dispersal of crusted fuel driven by internal pressures of a fraction of a MPa.) Subsequent

sequences of fuel collapse under gravity and dispersal are expected. Two sequences of collapse and eructation in L2 were not sufficient to produce fuel penetration past the 0.5-in. (1.27-cm) insulator-pellet region at either top or bottom of the fuel stack (see L2 radiograph in Fig. 1). However, because of the extensive mixing of molten fuel and cladding, it is expected that steel vapor will continue to be generated and will gradually "boil up" molten fuel into a continuing, dispersed, two-phase region, which could melt its way upward.

c. Movement of Standing Fuel. As noted in Sec. I, an LOF-triggered power burst would be expected to occur when the fuel throughout the cores sees a wide range of coolant conditions. At the time the "lead" fuel is slumping, other fuel subassemblies will still be intact, even though some coolant voiding will have occurred in some of them. The TOP test data provide guidance on the fuel motion to be expected to result from the response of this fuel to the power burst. Detailed analysis of the test conditions by mechanistic codes should be performed in order to extrapolate detailed test results to the actual LMFBR conditions, taking into account such differences as short test fuel and a relatively large ratio of test-coolant cross section to fuel cross section.

General, but not complete, fuel dispersal from the original location will occur, whether or not coolant is greatly subcooled or voided at the time of the burst. (In the latter case, dispersal may result from vaporization of residual sodium films on unheated structure.) The existence of the dispersal is clear from the tests, although there are potential uncertainties in modeling the details. Molten fuel ejected into liquid sodium tends to form fines, with mean size by weight typically of 200-500 μm; and this fragmented fuel appears to be readily dispersed. Some of the fines can plug gaps between cladding-tube remains.

Failure into an essentially voided channel (as in E4) produced a "flow-channel blockage" in the unheated regions at both the top and bottom of the original location of the fuel stack. Mild failure into heated, but subcooled, sodium produced a "blockage" above the top of the original fuel stack. Release of molten oxide at ~7200°F (4000°C) into subcooled sodium produced plugging by fines in the test sestion in channels between cladding-tube remains.

In none of the loop tests producing failure was there any "pure" benign fuel sweepout, that is, removal of hot fuel without freezing on cooler surfaces. Sweepout of some fuel into the loop was accompanied by extensive solidification of fuel or collection of fines within the general region extending between the top and bottom end fittings of the fuel pins.

2. Irradiated Fuel

a. Loss-of-flow induced Boundary Conditions Influencing Extended Fuel Motion. Direct postmortem inspection showed the existence of solidified stainless steel plugging at the inlet and outlet of the fuel region as a result of

the loss-of-flow sequence with irradiated fuel. The L3 and L4 fuel dispersals drove fuel upward beyond the location of the upper steel plug; however, the dispersal was not as extensive as that from overpower-failure loop tests (see the posttest radiographs from L3 and L4 in Fig. 1).

b. Movement of Melted Fuel. Available experimental data indicate that fuel collapse does not occur for irradiated fuel, since no collapse was observed in irradiated-fuel tests at burnups of ~4 at. %, even for the "high-power" L4 FTR fuel experiment. A single fuel eructation occurred in each of L3 and L4 during the power excursion. Timing of the irradiated-fuel eructations in L3 and L4 is consistent with the same mechanism as the first dispersal in L2. The reason for the absence of a postdispersal collapse and the occurrence of second eructations in L3 and L4 is not readily apparent. Some fuel debris penetrated the first few centimeters of unheated structure above the original top of the L3 and L4 irradiated-fuel structures.

It is suggested that delayed or "slow" dispersal of fuel beyond a thin top steel blockage is a viable mechanism, i.e., that fuel heated past the liquidus can disperse an initial blockage. In this case the sequence of events is as follows: Fuel melts during the power burst, and fission gas is released locally, voiding coolant channels of any remaining sodium and producing a gross dispersion inside the blocked region. Heat then is transferred from the fuel into the blockage until the latter is sufficiently weakened so that the internal pressure from released fission gases (or steel vapor) is sufficient to move the melting blockage and allow fuel to move upward.

This sequence of events actually parallels that generated in E7, in which molten fuel failed into voided channels, then slowly dispersed. The dispersal is predominantly upward, partly because of the axial thermal gradient and partly because gravity will tend to build up the inlet blockage to a thickness significantly greater than that of the outlet blockage. (This feature is consistent with the current modeling of molten-cladding motion by CLAZAS.) Dispersed fuel is frozen in place as it loses heat while moving upward through the colder structure. Because decay heat was not simulated in these tests, Figs. 1 and 2 do not show the full extent of upward fuel motion that could eventually occur.

c. Movement of Standing Fuel. Irradiated-fuel dispersal occurs whether or not the sodium temperature at the time of fuel failure is greatly subcooled (E3) or near saturation. As in the case of fresh fuel, mechanistic analyses should be performed to guide extrapolation of detailed test results to the detailed power histories of specific accident scenarios and thermohydraulics. The tests emphasized the behavior of higher-power fuel, which would induce accident response. Highly gassy fuel was used only in Test E3. The general picture summarized below, however, should apply to FTR, despite possible uncertainty in some details.

At ~50 ¢/s and near saturation (Test H5), limited fuel loss of geometry and dispersal is expected to occur. Fuel failure and movement are

expected to be consistent with the fuel solidus reaching into the equiaxed grain region; the subsequent fuel-dispersal mechanism may be vaporization of sodium present in the coolant channels when fuel is released, or it may be due to fission gas trapped inside the fuel structure. At ~3 $/s (Tests E6 and E7), the movement is expected to occur when the fuel solidus extends to the unrestructured region. The dispersal mechanism in this case may be sodium vapor, fission gas (probably with a slight delay short enough not to be apparent for the 1-s-period H5 power pulse, but long enough to be noticeable in the 200-ms-period power pulses of E6 and E7), or the vapor pressure of fuel or steel trapped in a fuel-steel mixture. The initial E7 dispersal is believed to have occurred into channels voided near the fuel top. Fuel movement was predominantly upward in the loop tests in accord with the axial thermal distributions. Some of the fuel moved several centimeters into the top unheated structure past the original top of the fuel stack. Neutron radiographs indicated that Test E7 produced a flow-channel blockage at the original top of the fuel stack, and a possible blockage at the bottom of the stack region (see the posttest radiographs of H5, E6, and E7 in Fig. 2).

C. Fuel Survival

From the tests considered here, guidance can be provided for analyzing how far into a given loss-of-flow accident a given class of fuel will survive. This summary is given below.

1. Loss of Flow

Timing of boiling inception and traces from test-section thermocouples indicate that calculations of temperature rises in the fuel are consistent with the data. (There are, however, no L-series pressure or flow spikes that have the sharp calculated signatures of pulses due to fission-gas release.) Failure predictions based on calculations of cladding-temperature rise until rupture due to plenum gas pressure occurs are probably reasonable. For many LMFBR accident cases, as well as the L and R tests described in Sec. III, the internal plenum pressure is low enough so that cladding rupture is not calculated to occur until after cladding dryout occurs.

The actual L2, L3, and L4 cladding conditions at the time of rupture are not known. Results are available from out-of-pile burst tests at HEDL on fresh and irradiated cladding. The HEDL test conditions may include larger amounts of gas than those actually available in the pins to do work on deforming the cladding after initial failure. If this is the case, the actual cladding distortion in the reactor may be smaller than that observed in the burst tests. Note that rupture of the fuel-pin cladding and fission-gas release do not indicate loss of coolable geometry. The melting of cladding, which then forms blockages (which do produce the loss of a readily coolable geometry), is recommended as the index of loss of fuel survival.

2. Power Burst Generated by Reactivity Insertion Caused by Loss of Flow

Although a detailed and comprehensive theory that quantitatively predicts failure threshold for power bursts has not been established, the available experimental data can be used to give experimental indices for failure of FTR-type fuel. In the assessment of survival, it is conservative to select failure indices that are below the experimental values,[2] so that pins which do not attain the selected levels for failure can be expected to survive. For convenience, we will discuss fresh fuel separately from irradiated fuel. For reviews of failure-threshold modeling done for the FTR, see Refs. 4 and 5.

Fresh fuel has been observed to fail by cladding meltthrough if that occurs before buildup of excessive internal pressure. Meltthrough has occurred after coolant boiling and dryout, and has also appeared to be the failure mechanism in Test E2, for a relatively cool sodium environment when a high melt fraction* and high average fuel temperature were attained. These criteria are noted in Table II.

TABLE II. Short-term FTR Fuel Survival during Power Burst

Fuel Type	Condition for Failure (only one required)
Fresh	80% fuel cross section at solidus or above.
	Cladding rupture calculated for internal pressure of fuel vapor.
	Coolant boiling (no superheat).
	Cladding temperature in excess of 2200°F (1200°C), to cover possible uncertainties in calculating meltthrough.
Irradiated	Fuel solidus reaches the equiaxed region.
	Cladding temperature high enough that previously released fission gas is calculated to cause failure.
	Coolant boiling (no superheat).

Irradiated fuel may be categorized by fuel structure, since fission-gas retention in the oxide matrix is a strong function of the microstructure. FTR-type fuel run at steady-state powers above 9 kW/ft (29.5 kW/m) will have a full developed radial microstructure consisting (from the center outward) of a central void, a columnar-grain region with low gas retention, an equiaxed region composed of inner (low gas retention) and outer (high gas retention) portions, and an unrestructured outer region with high gas retention. Failure has

*92% of fuel cross section at solidus or above.

been observed when the region calculated to be at the oxide solidus has extended to the relatively gassy fuel. These criteria are also given in Table II, with the H5 data taken for irradiated fuel and a possible heating-rate dependence not included.

3. Survival after Power Burst

Straightforward thermal calculations are recommended for calculations on fuel survival as intact pins after a possible power burst. The high heat content of some fuel that has fallen short of the transient thresholds given above can be expected to cause channel boiling and cladding melting in the low-flow conditions later in the loss-of-flow incident. Thus, calculation of the post-burst thermal conditions of unfailed fuel would be performed to check for continued survival. Criteria for the survival of the subassemblies should be the same as for the initial loss-of-flow phase. That is, fuel failure per se does not mark loss of coolable geometry within the subassembly. Rather, formation of channel blockages that prevent coolant from cooling the subassembly fuel is the real criterion.

For the small-size tests performed thus far, cladding melting and flow-channel blockages affected flow all across the test sections. Somewhat greater incoherence in failure and in postfailure blockage distributions would occur in a full-size subassembly.

D. Postaccident Fuel Condition

1. Reentry FCI

In none of the tests are there data to support the existence of an energetic fuel-coolant interaction (FCI) resulting from a postexcursion coolant-reentry event. Rather, the data show that the LMFBR conditions inhibit rapid vaporization and support analyses that predict a nonviolent heating of any returning sodium, whether or not the test was of a power-excursion or loss-of-flow type. The idealized "hard" reentry of a pistonlike mass of sodium followed by rapid mixing of fuel and coolant in the absence of vapor does not apply. The structure present at the conclusion of these experiments promotes incoherence of sodium return and impedes mixing.

Further, in such real systems there are local sources of vapor or gas, including vapor from incoherent sodium reentry on even the small scale of a few channels, gas trapped in the fuel (fill gas and gas from fabrication in the case of fresh fuel, and fission gases in the case of irradiated fuel), as well as vapor from fuel and/or structure. All these conditions tend to prevent rapid sodium vaporization. Note the low work conversions shown in Table I.

2. Fuel (Cladding) Locations and Conditions (Coolability)

Available data on the location and condition of solidified fuel and cladding at the end of the tests have been summarized above under categories

of types of incidents (e.g., loss-of-flow-produced boundary conditions for fresh fuel influencing extended fuel motion). Radiographs showing the macroscopic posttest conditions of fuel after six recent TREAT loop tests are given in Figs. 1 and 2. In general, they show that the immediate postburst or post-shutdown loss-of-flow experimental fuel distribution is predominantly one of relatively large solidified fuel masses in the general region of the original fuel stack. There is no dominant tendency to form readily cooled channels through these masses or to form debris beds.

However, the data described here refer to the condition after tests simulating power bursts or tests run at steady power for ~30 s with loss-of-flow phenomena. It may be expected that some of that part of the fuel that had been dispersed and frozen outside the fuel regions (note the plenum regions on the radiographs) would be readily coolable by returning sodium. The massive pieces of solidified fuel were solidified by the heat sink provided by the loop walls after TREAT power had been shut off. In the LMFBR, masses of molten fuel or fuel/steel/fission-product mixtures would still have power generation up to ~10% of steady power for tens of seconds after the nuclear shutdown produced by HCDA-generated fuel dispersal.

Under those conditions, those masses of internally molten fuel would stay hot, solid fuel could melt, gases would bubble through, and adjacent structure would melt, running down or floating to the top of the fuel. These considerations would support analytical models in which regions of dispersed fuel form, melting downward slowly through a lower steel plug or region below the fuel. The situation above this steel plug might be very dynamic. Steel vapor should play a role in movement of the fuel. The pool model should consider lateral growth by meltthrough of structure, vapor formation in the fuel and steel, and "boilup" of the fuel-steel mixture with corresponding upward meltthrough and pool growth.

Wherever molten fuel comes into contact with sodium, extensive fragmentation will result. Because of the physical properties of solid fuel, extensive fragmentation should also occur whenever hot solid fuel comes into contact with cooler sodium.

Another important aspect in this area is the quantity of material carried away from the original core region. In one particularly favorable case with highly subcooled bulk sodium, and a very high ratio of sodium volume to coolant volume (Test E2), extensive quantities of fuel fines were carried from the test section. About 40% of the fuel was found in the loop outside the test section in the form of fines.

In none of the seven-pin Mark-II loop tests described here did neutron radiographs show evidence of large quantities of fuel fines (i.e., equivalent to ~10 g) outside the test section. Multigram quantities of fines comparable to those generated and carried out of the test-section region in E2 were not carried out of the test-section regions of the Mark-II loops in the seven-pin tests.

Samples of sodium taken from loop regions outside the test section did show plutonium contamination large enough to be measured. These were typically of the order of tens of ppm, although one reading from E7 was ~500 ppm. Note that the samples from irradiated-fuel tests were taken inside an alpha-gamma hot cell, so it is conceivable that some of the plutonium measured may have come from other sources. For orientation, an average of 10 ppm plutonium in the loop sodium corresponds to ~0.01 g of plutonium total released from a test cluster of fuel pins containing ~100 g of plutonium. This represents a total carryout of ~0.01%. If the high E7 datum is taken as an upper limit, then it would correspond to 0.5% carryout.

III. CONDENSED TEST SUMMARIES

The transient tests used for this assessment are reported elsewhere. References are given at the end of this report. For clarity, condensed test summaries are included here to provide a basis for this assessment. Each test is summarized once, listed in the category into which it appears to fit best. Results from a single test may, of course, be applicable to two or more categories; and inclusion of a test under its "principal" application is not intended to imply that it is not relevant to other cases. The tests by "principal categories" are listed in Table III.

TABLE III. Test Listing by Categories

A. Extended Fuel-Cladding Motion Resulting Directly from Loss of Flow

1. Loss-of-flow Tests with Fresh Fuel

a. Fresh-fuel Loop Test L2
b. R-series Loss-of-flow Tests
c. Capsule Tests at Petten

2. Loss-of-flow Tests with Irradiated Fuel

a. "Intermediate-Power Structure" (PNL-17) Pins in Loop Test L3
b. "High-Power Structure" (HEDL-N-F) Pins in Loop Test L4

B. Extended Fuel Motion Resulting Directly from a Power Excursion Produced by Fuel Slumping Caused by Loss of Flow

1. Fresh Fuel

a. Fuel Failure into Greatly Subcooled sodium
(1) Loop Test E2
(2) Autoclave Tests S11 and S12
(3) Electrical "Exploding" Fuel-pin Test
b. Fuel Failure into Subcooled Sodium Approaching Saturation
(1) Loop Test H2
c. Fuel Failure into Voided Channel
(1) Loop Test E4

2. Irradiated Fuel

a. Loop Test E3
b. Loop Test E6
c. Loop Test E7
d. Loop Test H4
e. Loop Test H5
f. Capsule Test C5A
g. Capsule Test C5B

C. Fuel Survival in Power Bursts

D. Postaccident Fuel Condition: Autoclave Tests S2-S8

A. Extended Fuel/Cladding Motion Resulting Directly from Loss of Flow

1. Loss-of-flow Tests with Fresh Fuel

a. Fresh Fuel (Seven PNL-17-type Pins) in Loop Test L2.[1,6,7]

Seven fresh fuel pins with 13.5-in. (34.3-cm)-long fuel columns were run in a Mark-II-loop loss-of-flow simulation in Test L2. After an initial sample power of 18 kW/ft (59 kW/m) to accelerate attainment of steady-state-like

temperature profiles, the sample power was lowered to 11 kW/ft (36 kW/m) and the flow was reduced to produce boiling. Sodium dryout, cladding melting, and fuel slumping followed. As shown in Fig. 1, stainless steel was found plugging the channels between pins at both the top and bottom of the initial fuel-stack region. Fuel, containing solidified-steel droplets dispersed widely through it, was concentrated above the solidified steel at the bottom, and a much smaller amount of fuel was concentrated below the upper solidified steel. Steel solidification at the top appeared to occur predominantly at the 0.5-in. (1.3-cm)-long upper natural UO_2-insulator-pellet region. The bottom steel blockage was located at the 0.5-in. (1.3-cm)-long lower natural UO_2-insulator-pellet region and extended more than an inch into the 3.375-in. (8.57-cm)-long bottom-end-cap region.

Evaluation of transient flowmeter and thermocouple data indicated that the first stainless steel melting occurred about 4 s after boiling began. Plugging, as noted by abrupt cessation of inlet and outlet flow oscillations, occurred ~0.7 s later. Fuel-motion data from the hodoscope showed oxide slumping (significantly slower than free fall) to begin about 1 s after plugging. Slumping was complete after about 0.5 s, and the fuel then remained essentially quiescent for about 4 s, after which--about 11.3 s after boiling began--fuel dispersed (upward), followed by another collapse. A second dispersal--followed by collapse--occurred about 1.8 s after the first.

The quiescent period represented a nominal energy input ~800 J/g of oxide at the nominal power level of 11 kW/ft (36 kW/m). This energy is sufficient to raise the temperature of oxide (under adiabatic heating) to ~3800 or ~4400°C from the solidus or liquidus, respectively. A lower temperature--say ~3300°C--may be estimated, due to the axial neutron filters and to increased self-shielding of the slumped fuel. At this temperature, the fuel vapor pressure would not be a candidate for the source of the pressure causing the dispersal. A source of pressure considered more likely for the observed dispersals would be the vapor pressure of steel constituents. This pressure is estimated to be 1 atm (1×10^5 Pa) at the oxide melting point and about 6 atm (6×10^5 Pa) at 3300°C.[8]

Flow could not be reestablished through the test section after the test, a result consistent with the fuel/cladding conditions observed afterward.

Samples of sodium were taken from the L2 loop during the glovebox operations of loop disassembly and were analyzed for plutonium contamination of the sodium in ppm (μg Pu/g Na). Results were as follows: at the top of the pump, 328 ppm; at the bottom of the pump, 283 ppm; and in the bottom bend below the test section, 278 ppm. Measurements indicated that "background" contributions to these numbers were <10%.

b. R-series Loss-of-flow Tests.[3,9] R-series loss-of-flow tests are being conducted in the TREAT reactor using a special once-through loop designed for full-length FTR-type fuel pins and providing a mockup of key FTR

boundary conditions in the axial directions. Three tests were performed before July 1974, all with constant power. In each test, sodium flow was established prior to the reactor transient by a pressure differential between supply and receiving tanks. Then, after typical steady-state thermal conditions had been achieved in the test section in the early part of the power transient, the pressure difference was reduced to provide the loss of flow. In each of the first three tests, average pin power was 10 kW/ft (32.8 kW/m).

(1) Test R3. Test R3 was conducted with a single pin to check single-pin voiding. Power continued for 12.25 s after boiling inception. Cladding dryout was indicated 2.35 s after boiling, and a flow anomaly interpreted as gas release from the pin, followed at 3.35 s after boiling. The fuel-stack length within the 20-in. (52-cm)-long hodoscope viewing window did not collapse during the test. This was consistent with radial heat loss to the structure, which was calculated to be adequate to prevent complete fuel melting. Posttest neutron radiographs showed an extensive steel plug at the base of the pin, but no clear evidence for a possible downstream plug at the top. No data indicating an FCI were observed.

(2) Test R4. Test R4 was run with seven pins. Power continued for 11.75 s after the inception of boiling. Cladding dryout was indicated 1.95 s after boiling began, and evidence of gas release due to cladding failure occurred 2.75 s after boiling inception. Flow-tube thermocouples showed evidence of upward movement of molten cladding ("flooding") about 1 s later, followed by formation of an exit blockage. Hodoscope data were lost by the developer. Posttest neutron radiography showed an extensive steel plug at the bottom of the fuel in the region of the Inconel bottom reflectors. There was no indication of fuel penetration past this plug. Extensive fuel collapse upon the steel plug was apparent, with the collapsed region extending upward about 15 in. (38 cm). There was a thin downstream plug of solidified steel located at the region of the upper insulator pellets. No FCI events occurred.

(3) Test R5. Test R5 was terminated 5.75 s after the R4 time of boiling inception in order to obtain better postmortem data on the details of early cladding motion. Timing of flow events and the movement of molten steel were comparable to those for R4. The hodoscope data showed no gross fuel collapse during the power transient. However, the hodoscope did show an abrupt downward "snaking" motion from the upper part of the original fuel region into the central region, occurring about 1 s after scram. The posttest neutron radiography showed slumped regions of pellet-like fuel debris above and below a central region of deformed fuel "cylinders." The upper steel blockage at the upper insulator-pellet region was relatively thin, as in R4; the lower blockage was much thicker. No FCI events occurred.

One aspect of the lower steel blockages observed in R4 and R5 should be clarified here. The R loops have steel heat sinks attached outside the lower portion of the primary-loop wall in the region of the test section,

in order to prevent a possible meltthrough of fuel in the event of a test accident. These heat sinks are not in contact with the test trains or flow channels and thus cannot influence any premature freezing of steel running down within the test section. Transient-heat-transfer calculations showed that heat loss to the outside of the loop wall occurred on a longer time scale than that required for steel to freeze on the bottom end fittings of the fuel.

c. Capsule LOF Simulations at Petten.[10,11] Single-pin-capsule loss-of-flow simulations with samples containing 10-in. (25-cm)-long fuel stacks are being performed at the Reactor Centrum Nederland, Petten. In these tests, the heat from the test pin is conducted radially to cooling water through a sodium annulus inside an independent NaK annulus. Radial heat flow can be interrupted to simulate a loss of cooling event by programmed removal of the NaK. The test reactor is scrammed at a prearranged time after the start of the "loss of cooling."

(1) Test LO3. The loss-of-cooling time of 9.6 s was selected to provide about 1 s of power after initiation of sodium boiling. The rate of sodium temperature rise during this period was ~140°F/s (78°C/s). Some central fuel melting occurred, without producing slumping of the fuel remains. Cladding melted over about a 6-in. (15-cm) length. No annular blockage of the coolant channel by solidified stainless steel occurred.

(2) Test LO4. The loss-of-cooling time for Test LO4 was set to provide about 5 s of continued power after boiling inception. The average rate of temperature rise of the sodium annulus before boiling was about 117°F/s (65°C/s). Neutron radiography showed the posttransient condition of the sample. Cladding melted over about an 8-in. (20-cm) length. The fuel column had disintegrated over the length of one pellet, with the release of some molten fuel which solidified in the annular coolant region. There again was no indication of slumping of the fuel remains. However, the radiographs showed a concentration of solidified material in the sodium annulus, near the bottom of the fuel stack, which could correspond to a channel blockage.

(3) Test LO5. The loss-of-cooling time was set at 14.5 s, providing several seconds of power after boiling initiation. The average rate of coolant temperature rise was ~64°C/s. The cladding had melted off and run down, except for a few areas in which steel lumps bridged the gap between fuel and structure, and froze in place. A thin-walled fuel column remained standing. It was found bulged near the bottom, apparently as a result of the hydrostatic pressure of internal molten oxide acting on the plastic, high-temperature oxide wall. Evidence of a few small jets of molten oxide from the pin was found near the bottom. A pressure pulse of 12 atm (1.2 MPa) was recorded. (The pulse was broad, with 850-ms half-width.) This pulse is consistent with nonviolent boiling of a small quantity of sodium remaining in the bottom of the capsule after some molten fuel dropped down.

(4) Test LO6. Test LO6 was run with a pin prepressurized to 75 atm (7.5 MPa) at room temperature. It was deliberately run just short of failure, with a loss-of-cooling time of 6.25 s.

(5) Test LO7. Test LO7 was scrammed (apparently on an experiment pressure signal) at 6.7 s, after cladding failure. The release of gas blanketed the cladding pin, interrupting heat flow, and resulting in extensive cladding melting. The maximum pressure recorded was 160 atm (16 MPa). It was attributed to the release of the relatively cold gas from the pin plenum and its subsequent heating due to contact with the high-temperature materials inside the capsule.[12] The average rate of coolant temperature rise was 83°C/s.

(6) Test LO8. Test LO8 was a rerun of Test LO5. Test conditions were essentially the same (loss-of-cooling time of 13.8 s and sodium heating rate of 65°C/s). Results were comparable, except that there was no pressure pulse.

2. Loss-of-flow Test with Irradiated Fuel

a. "Intermediate-power Structure" (Seven PNL-17) Pins in Loop Test L3.[1,13-15] Loss-of-flow Test L3 was conducted in essentially the same fashion as Test L2, using fuel irradiated to about 3.5 at. % burnup, with an intermediate-power structure. The initial sample pulse was 15 kW/ft, (49.2 kW/m) and the subsequent steady-state level was 9 kW/ft (29.5 kW/m). As in L2, the test was carried past melting and produced a fuel-dispersal event.

Posttransient radiographs of L3, reproduced in Fig. 1, showed extensive removal of fuel from the midregion of the original fuel column and displacement of failed fuel extending upward several inches from the original top of the stack. Some debris appeared to be in the bottom bend. This debris was collected and found to be about 1.3 g, only part of which was fuel.

Small quantities of fuel were found along the fuel plenum region, both within the cladding and in the coolant channels. Thermocouples near the top of the fuel stack, located on the flow tube, indicated the presence of molten steel (or possibly contact with fuel) about 5 s after boiling began. No clear flow anomalies indicating L2-like buildup of flow/void oscillations occurred, and hence there was no L2-like cessation of flow oscillations indicating the timing of flow-channel plugging.

About 14.2 s after boiling began, both upper and lower flowmeters showed expulsion, ~7 m/s upward and ~5 m/s downward, respectively. This expulsion event is correlated with a 15-atm (1.5-MPa) pressure spike on the lower pressure transducer and hodoscope detection of a general upward expulsion of the upper half of the fuel. This expulsion was largely complete in 0.15 s. There was no fuel collapse either before or after the expulsion.

Flow could not be reestablished after the experiment, a result consistent with the fuel agglomerations seen in the posttest radiographs. Note that each PNL-17 irradiated pin used in L3 had only a thin welded steel spacer tube above the 0.5-in. (1.27-cm)-long UO_2 insulator-pellet section at the top of the fuel stack, while each L2 pin had an Inconel rod. Although the L3 pins had less heat sink above the fuel, this fact appears inadequate to explain the upward penetration of some fuel debris within the L3 plenum, as compared with L2, since the stainless steel blockage in L2 occurred in the insulator-pellet region below the Inconel.

There were no sharp flowmeter-pressure transducer signals like those from SAS calculations of fission-gas release during the time that test-train thermocouples indicated that cladding failure occurred; rather, the data indicate a slower release of the plenum gas. Dispersal is attributed to the same phenomenon that caused the first fuel eructation in L2.

The postmortem inspection showed that the upper stainless steel blockage was located just above the original top of the fuel column. The fuel column appeared to have small channels through it. Fuel debris and steel globules were found above the blockage. Globules of stainless steel were found in various degrees of dispersion in sections of solidified fuel, in the approximate range of 1-5 areal percent. Some regions of solidified fuel were found that appeared to be free of metallic particles.

During the sectioning of the L3 loop, sodium samples were taken from the regions where the loop was separated and the plutonium concentrations measured. Results were as follows: at the top of the pump, 18 ppm plutonium (18 μg/g of sodium); at the bottom of the pump, 1 ppm plutonium; and just below the bottom of the test section, 0.5 ppm plutonium.

b. "High-power Structure" (HEDL-N-F) Pins in Loop Test L4.[1,13,14,16] Test L4 was similar to Test L3, except that the sample pins were "high-power structure" irradiated samples. The sample steady-state power in L4 was 10 kW/ft (32.8 kW/m). Posttransient radiographs (see Fig. 1) show concentrations of failed fuel similar to those of L3, except that there appears to be somewhat more upward fuel movement than noted in L3. Thermocouples along the flow tube indicated the presence of molten steel (or possibly contact with fuel) about 5.5 s after evidence of boiling was seen on flowmeters and a thermocouple on the flow tube near the top of the fuel. No clear flow signals indicating oscillations occurred; hence there was no L2-like cessation of flow oscillations indicating the timing of blockage.

Radial expansion of the fuel mass also began about 5.5 s after boiling inception. This expansion appears to have a maximum extent to the limits imposed by the loop, i.e., consistent with pushing the flow tube outward until it contacts the massive loop wall proper.

About 13.5 s after boiling began, there was a rapid explusion of fuel upward from two main sites: one about a third of the way up from the bottom of the fuel, and one two-thirds of the way up. Some net fuel movement toward the axial center was noted. However, this did not raise the fuel density above the original value. This event merely "replenished" an earlier, small, local loss of fuel which had moved downward from the center of the column. This expulsion lasted about 70-ms. It was correlated with coolant expulsion at a rate of ~5 m/s as recorded by the inlet flowmeter and with a 5-atm (0.5-MPa) pressure spike on the lower pressure transducer.

A milder flow event, with no associated pressure pulses, occurred about 18 s after boiling began--which is about 1.1 s after the transient was scrammed. Flow could not be reestablished after the test. As in L3, there were no clear "signatures" of sharp flow and pressure anomalies like those of SAS calculations of fission-gas release. The fuel-expulsion event occurred ~13 s after boiling, at ~13 x 10 kW/ft (32.8 kW/m) = 130 kJ/ft (426.5 kJ/m), and is attributed to the phenomenon producing the first eructation in L2.

Plutonium concentrations in L4 loop sodium samples were as follows: at the top of the pump, 5 ppm plutonium; at the bottom of the pump, 48 ppm; below the bottom of the test section, 0.5 ppm.

B. Extended Fuel Motion Resulting Directly from Possible Power Excursion Produced by Fuel Slumping Caused by Loss of Flow

1. Fresh Fuel

(a) Fuel Failure into Greatly Subcooled Sodium in Loop Test E2.[2,17-19] Test E2 was performed with a single UO_2 pin inside a ring of six hollow dummy pins. The primary goal of this test was to study the phenomena associated with a high-energy oxide-pin failure in relatively cool bulk sodium in a flow channel (i.e., loop) geometry, permitting sodium expulsion and reentry. Test E2 was the first TREAT loop test in which an oxide pin was failed under overpower conditions. The test pin failed when about 90% of the fuel cross section by area was at the oxide solidus or above. The maximum fuel temperature at the time of failure was ~7200°F (~4000°C).

Because of the test-section geometry (one fueled pin in a ring of six dummy pins), the bulk sodium temperature was relatively cool, ~860°F (460°C), at the time of failure. Extensive fuel fragmentation and dispersal occurred. About 75% of the fuel was recovered after the test in form of fines, ~50% from the test section and the remaining fines from the remainder of the loop. Approximately half the fines from both populations, by weight, were particles of less than 200 μm.

Although there were no dense plugs of solidified fuel or cladding, sodium flow could not be reestablished after the test. The flow blockage

was caused by fuel fines packed between the cladding remains in the test section. Careful examination of the fuel residue left inside the cladding of the fueled pin showed that fill gas was trapped between the fuel and cladding, from whence it was forced toward the molten center of the fuel stack, where it could act as a mechanism for expelling fuel. Essentially all the fuel cross section had reached the solidus, on the basis of the structures of these remains. Analysis of the coolant-motion data indicated that work done on the coolant was ~1 J/g oxide.

(1) Autoclave Tests S11 and S12.[20,21] Autoclave tests S11 and S12 were run with single fresh pins inside a sodium annulus, contained within a molybdenum heat sink. Test conditions and design were selected so that the thermal conditions at failure were representative of those for a prompt critical LMFBR accident; i.e., there were a high internal oxide vapor pressure and low sodium temperature. Maximum oxide sample power in both tests was ~15,000 cal/g·s (64,000 W/g). Test data are summarized in Table IV.

TABLE IV. Summary of Test Data for Tests S11 and S12

Event	S11	S12
Exterior cladding temperature calculated at time of failure, °F (°C)	1350 (730)	990 (530)
Sample energy at failure, J/g	3130	3130
Total sample energy, J/g	6760	6760
Maximum pressure pulse, atm (MPa)	136 (13.6)	68 (6.8)
Energy conversion to work on autoclave piston, J	~20	≤20
Specific energy conversion, J/g oxide	~1	≤1
Mass mean size of fuel fines, μm	155	110

(2) Electrical "Exploding" Fuel-pin Test at Atomics International.[22] Molten UO_2, generated by an electrical power burst in an internally insulated fuel pin, was released into a sodium "pipe" test section with expansion tank above. Bulk coolant temperature at the time of the release was about 1200°F (650°C). Extensive fragmentation of the oxide occurred. Half of the fines by weight had sizes below 400 μm. Sample electrical energy input was ~4000 J/g. Work done on the coolant was ~125 J total compared with a total electrical energy input to the pin of ~36,000 J for an energy conversion of 14 J/g oxide.

b. Fuel Failure in Subcooled Sodium Approaching Saturation in Single-fresh-pin Loop Test H2.[2,23,24] Test H2 was run with a single, FTR-type pin in an unshaped TREAT transient programmed to carry the pin just to the anticipated failure-threshold region. The power-pulse duration at half-maximum was about 315 ms. The test pin failed with ~76% of the fuel cross section at the solidus or above and a maximum fuel temperature of 5650°F (3120°C). The maximum bulk coolant temperature calculated at the time of

failure was about 1470°F (800°C). The maximum calculated rate of temperature rise at the cladding midpoint was about 3760°F/s (~2070°C/s).

Neutron-hodoscope data showed that before failure, fuel was moved upward about 1.5 in. (3.8 cm) inside the cladding, creating a low-density region in the top third of the fuel stack. A partial return and a second upward expulsion of fuel occurred before failure was indicated by flow and pressure anomalies. This internal expulsion and reentry provide a mechanism of failure at a local "hot spot" in which upward fuel expulsion opens a path from the fuel interior to the cladding and places molten fuel against the cladding.

Analysis of the flow data indicated that local boiling occurred for about 50 ms prior to failure. The posttransient fuel-stack remains consisted of a thin-walled "chimney" for the bottom two-thirds of the original length. The chimney walls were consistent in thickness with the calculation of the thickness of fuel below solidus at failure. The fuel expelled from this chimney and from the top third of the stack (the initial failure appears to have occurred within the top inch of the fuel stack) was solidified above the original location of the fuel stack and packed around the fuel plenum inside the single-pin fuel holder.

About three-fourths of the original fuel was recovered from the test section in the form of fines. Approximately half of these fines were found typically to contain 0.5 vol % of dispersed solidified steel. Work done on the coolant was ~0.15 J/g oxide.

c. Fuel Failure into Voided Channel in Single-fresh-pin Loop Test E4.[2,24,25] The E4 sample and test-train design were the same as for H2. The TREAT power pulse, however, was more severe, being intended to carry the pin well beyond the failure threshold. Pin failure occurred when essentially the full fuel cross section was at the liquidus or above. Maximum calculated fuel temperature at this time was 6550°F (3620°C). Failure was indicated after voiding of the top 11 in. (27.9 cm) of the coolant channel adjacent to the 13.5-in. (34.3-cm)-long fuel stack. Local boiling was indicated for about 40 ms prior to failure. The calculated rate of temperature rise of the midpoint of the cladding near the top of the E4 pin at the time coolant boiling began was ~8000°F/s (~4400°C/s).

Extensive fuel movement occurred; one agglomeration of fuel, insulator pellet, and cladding particles was found at the bottom end plug. Some of the fuel had been frozen onto the structure in the original region of fuel, but most of the fuel had been moved upward into the plenum. A substantial flow blockage consisting of solidified fuel and cladding was located about 3.5 in. (8.9 cm) above the original top of the fuel column.

Some fuel fines were collected during the test-section disassembly; these contained up to 10 vol % of stainless steel. About 1 g of debris--mainly light-density material--was collected from the loop sodium. Thus an

upper limit of 1 g can be set for fines sweepout from the test section. In general, solidified fuel contained dispersed solidified steel particles amounting to a few volume percent. Work done on the coolant was estimated to be ~0.85 J/g oxide.

2. Irradiated Fuel

a. Loop Test E3.[2,26] Test E3 was an early survey test run in the loop in order to check the order of magnitude of conversion of thermal energy to work for irradiated oxide fuel. The test sample consisted of three small-diameter UO_2 fuel pins irradiated to a maximum burnup ~6 at. %. Failure about 5 ms before the hottest fuel reached it solidus was indicated by pressure and flow anomalies occurring when the hottest pin had received a radially averaged energy input of about 855 J/g. Maximum bulk coolant temperature at the time of failure was calculated to be about 1050°F (565°C). Maximum pressure observed was ~58 atm (~5.8 MPa) at the outlet. Maximum pressure from the inlet transducer was about 34 atm (3.4 MPa). Estimated internal gas pressure at the time of failure due to fission gas released before the test into the plenum was ~30 atm (~3 MPa). Hodoscope data indicated that the motion of the fuel was relatively gradual in the upward direction and was essentially complete in about 100 ms.

Extensive final dispersal of the fuel from the original fuel region was found. Most of the fuel was removed into the loop. About one-third of the fuel was piled up in the form of fuel fragments on the thermocouple-holder fixture above the pins. Following the test, the flow was found to be completely blocked. This test produced the largest conversion of thermal energy to coolant kinetic energy per gram of fuel of any TREAT loop test.

Total conversion was calculated to be about 150 J, or 4 J/g-oxide, which includes work done by expansion of released fission gases. An upper limit of ~100 J was estimated as due to expansion of all fission gas (including that trapped in the oxide). Thus, the net conversion from sodium vaporization is estimated as ~3 J/g oxide.

b. "High-power-structure" (HEDL-N-F) Pin inside Ring of Six Fresh Pins in Loop Test E6.[2,13,27,28] The Test E6 power pulse was programmed to simulate a 3 $/s excursion. The "high-power-structure" pin was contained inside a ring of six fresh "environmental" pins. The reactor period in E6 was about 188 ms, and the power-pulse half-width was ~250 ms. Flow and pressure data indicated that fuel failure occurred when the irradiated central pin had about 80% maximum of the fuel cross section at the solidus or above, essentially all of the fuel in the hottest peripheral (fresh) pin had reached the solidus, and the maximum calculated bulk coolant temperature was 1750°F (954°C).

Maximum rate of temperature rise of the cladding midpoint was about 2100°F/s (1150°C/s) for the irradiated pin. (The columnar and equiaxed regions extended outward to about 65% of the cross section.) Maximum temperature in the central irradiated pin at the time of failure was about 6000°F (3316°C). Flow could not be reestablished after the test.

Neutron radiographs (see Fig. 2) showed fuel-column remains in the region originally occupied by fuel. A bulging hollow section of fuel remains was located between 10 and 12 in. (25-30 cm) from the bottom of the fuel region. Failed-fuel remains were distributed extensively over a length extending about 10 in. (25 cm) above the original location of the top of the fuel.

One of the fresh-fuel pellets near the top of the fuel column showed evidence of molten stainless steel intrusions into peripheral "startup" cracks and small globules of steel near the intrusion. Once-molten fuel from a sample location about 2.25 in. (5.2 cm) above the original bottom of the fuel stack showed finely dispersed steel globules.

c. "High-power-structure" (HEDL-N-F) Pins in Loop Test E7.[2,13,29,30] The E7 power pulse was programmed to approximate a 3 $/s excursion for a cluster of seven "high-power-structure" pins. Reactor period was about 180 ms, and the power-pulse half-width was about 310 ms. No sharp flow or pressure anomalies occurred during the E7 transient. Two "failure" references can be established near peak power by timing of the flow anomalies. The first was a mild surge suggesting release of a fission-gas bubble, and the other a mild sodium ejection occurring about 100 ms later. The first event began when the solidus in the hottest of the seven irradiated fuel pins was calculated to have reached the middle of the equiaxed region. At the time of voiding, the solidus had reached the boundary of the unrestructured fuel. (The columnar and equiaxed regions extend outward to about 65% of the cross section.)

Flow could not be reestablished after the test. Work done on the coolant was about 0.3 J/g oxide. Neutron radiographs (see Fig. 2) showed no structure reminiscent of the original seven fuel stacks. Fuel remains were smeared over the bottom 5 in. (12.7 cm) of the original fuel region, and some fuel fragments were found spread through the bottom 0.5-in. (1.3-cm) insulator-pellet region and about 1.5 in. (3.8 cm) into the bottom-end-plug region. Relatively dense fuel extended upward to about 3 in. (7.6 cm) into the UO_2-blanket pellet region beyond the location of the pretransient top of the fuel, and additional fuel fragments were scattered through another 6.5 in. (16.5 cm) to within about 2 in. (5 cm) of the top of the Inconel reflector rod.

Neutron-hodoscope data showed a slow fuel motion beginning approximately at the same time as the sodium ejection event. Fuel motion eventually resulted in voiding fuel principally upward from the axial central several centimeters of the test section. The motion was not complete 0.6 s after peak power. At this time, power had dropped to a magnitude comparable to preheat.

Postmortem inspections showed that the region extending upward from about 3 in. (7.6 cm) above the original top of the fuel to about 5.25 in. (13.3 cm) above was held together by steel which had been pushed up from below in the molten state and then had frozen. Globules of stainless steel were found extensively dispersed throughout the solidified fuel. These globules were typically present at the level of a few volume percent.

Plutonium concentrations in E7 loop sodium samples were as follows: at the top of the pump, 0.2 ppm; at the bottom of the pump, 492 ppm; and just below the bottom of the test section, 0.3 ppm.

d. "High-power-structure" (HEDL-N-F) Pin inside Ring of Six Fresh Pins in Loop Test H4.[2,31] Test H4 was conducted with a single "high-power-structure" pin inside a ring of six "environmental" fresh pins. The power pulse simulated a 50 ¢/s-ramp FTR hypothetical accident. The reactor period was about 1 s. Test hardware and initial conditions were matched to Tests E6 and H5 to facilitate comparison of effects of fuel structure (H4 versus H5) and energy-rise rates (H4 versus E6). Pin failure was marked by pressure pulses of ~10-atm (~1-MPa) amplitude. At this time, the maximum calculated cross section of fuel at the solidus or above in the irradiated pin at the height of failure was about 20%, somewhat less than the area of the columnar region at that height.

Flow data show partial voiding of the coolant channels after failure. Evaluation of the data suggested that a flow blockage formed near the top of the fuel column about 0.1 s after failure. About 330 ms after failure, the hodoscope indicated extensive fuel movement. As coolant reentered the voided region, about 500 ms after failure a "reentry" event produced a 70-atm (7-MPa) pressure spike. No evidence was found for energetic sodium-vapor events.

The total work done was about 100 J. After the test, about 10% of the initial flow could be reestablished through the test section. Post-test neutron radiography showed the fuel to be nearly destroyed over the upper 85% of the original fuel-stack length. Most of the fuel appeared to have moved upward, almost filling the test-section cross section over a 4.5-in. (11.4-cm) length at the top of the initial fuel region. Additional fuel debris was at the bottom of the region.

e. "Intermediate-power-structure" (PNL-17) Pin inside Ring of Six Fresh Pins in Loop Test H5.[2,13,32,33] Test H5 was conducted with a single "intermediate-power-structure" pin inside a ring of six "environmental" pins. The power pulse simulated a 50 ¢/s ramp. The reactor period was about 1.1 s, and the pulse half-width was about 1.0 s. Pin failure was marked by pressure spikes on both pressure transducers and a sodium-expulsion event on the upper flowmeter. At that time, calculations showed the extent of fuel at the solidus or above in the central irradiated pin to be about 10% of the cross section at the height of failure. (Columnar-region maximum was about 15% of the cross section.)

The maximum calculated rate of temperature rise for the cladding midpoint of the irradiated pin was 350°F/s (194°C/s). In the hottest of the six fresh peripheral pins, about 55% of the fuel cross section was calculated to have reached the solidus. Maximum temperature in the central pin at this time was 5000°F (2760°C). The maximum calculated bulk-coolant temperature was 1300°F (703°C). Peak pressures measured were 10 atm (1 MPa) (upper transducer) and 17 atm (1.7 MPa) (lower transducer). Only 40% of the original flow rate could be established after the test. Neutron radiographs (see Fig. 2) showed damage to be concentrated about 3 in. (7.6 cm) above the center of the fuel stack. Some fuel remains were found above the original top of the fuel stack, extending upward over about 10 in. (25.4 cm).

Posttest macroscopic examinations showed the central-pin cladding to be breeched over a small area located about 5 in. (12.7 cm) above the fuel midplane. The peripheral pins had experienced extensive cladding melting and some loss of fuel. Little fuel was lost from the central pin. Evaluation of the posttest examination data indicated that the central pin failed first, but the possibility that one or more peripheral pins failed first could not be excluded. Hodoscope data indicated limited fuel motion attributable to voiding of individual pins, with fuel movement from the pin lateral and upward.

Plutonium concentration in H5 loop sodium samples were as follows: at the top of the pump, 1 ppm; at the bottom of the pump, 32 ppm; just below the bottom of the test section, 0.8 ppm.

f. GE Capsule Test C5A with a "Low-power-structure" Pin.[34] A single "low-power-structure" pin was irradiated in TREAT in the stagnant-sodium capsule Test C5A. Pin failure resulted from a transient that was calculated to raise ~35-40% cross section of the fuel to the solidus or above. The pin had been irradiated previously to ~2 at. % burnup at a maximum oxide temperature calculated to be below 3000°F (1650°C). Maximum temperature calculated (assuming no failure) in the NaK annulus outside the cladding was about 850°F (455°C). The sample failed extensively, with fuel movement into the coolant annulus extending upward to about 3 in. (7.6 cm) above the upper fuel-blanket interface.

A cross section through the failure region showed a solidified "clinker" filling the space inside the capsule. The remains of the fuel column were essentially a stack of hollow oxide cylinders, no longer in a straight column, but not slumped, either. Molten cladding had run down and solidified locally, with no evidence of molten-cladding dispersal, fragmentation, or collection into solidified agglomerations. Maximum sample power was ~555 cal/g·s (~2320 W/g).

g. GE Capsule Test C5B with a "Low-power-structure" Pin.[34] Test C5B was nominally the same as C5A, except that the C5B sample contained an annular upper blanket. Pin failure did not occur. A bulge in the

cladding was found in the region of the fuel-blanket interface; at this spot, pellet separation had occurred, and molten fuel had made contact with the cladding. Elsewhere, the nominal fuel maximum cross section at the solidus or above was ~35-40%. Maximum fuel temperature was ~5500°F (3020°C), and maximum temperature in the NaK annulus adjacent to the cladding (remote from the localized contact with molten fuel) was ~850°F (455°C). Extensive motion of molten fuel from the 24-in. (61-cm)-long fuel stack into the annular upper blanket occurred.

Maximum extension of fuel into the 0.070-in. (0.178-cm)-dia blanket central hole was about 10 in. (25.4 cm). The volumetric expansion indicated by this 10-in. (25.4-cm) travel is, however, quite small (~4%). Since about 35% of the fuel was calculated to be carried through the heat of fusion, the expansion into the blanket corresponds to ~12 vol % expansion of the fuel that became fully molten. The maximum fuel temperature during steady-state irradiation (to ~2 at. % burnup) was calculated to be less than 3000°F (1650°C).

Less than 10% of the fission gas generated in the steady-state irradiation was calculated to have been released before the transient; after the transient, however, about 44% gas release was measured. Thus, this test illustrates a relief mechanism to prevent failure and the ability of well-cooled cladding to contain local concentrations of molten fuel. It does not support explosive expansion of molten "gassy" irradiated oxide to a low-density form during an overpower transient with maximum sample power of ~555 cal/g·s (2320 W/g).

C. Fuel Survival in Power Bursts

See Sec. III.B above.

D. Postaccident Fuel Condition: Autoclave Tests S3-S8[21]

A series of autoclave TREAT tests was conducted using small clusters of oxide-fuel pins immersed in stagnant sodium in order to study the phenomenology and kinetics of rapid sodium vaporization (FCI). In none of these tests did an energetic FCI occur. Sharp, individual pressure pulses were observed, but these did little mechanical work, and there was no evidence of a general, coherent FCI involving a sizable fraction of the fuel inventory. The largest pressure pulse was about 200 atm (20 MPa) in magnitude, but the work associated with it was very small. Table V presents summary data. In one test, S5, the pins were evacuated in order to check the effects of internal gases. In all other tests, the pins contained inert fill gas at ambient pressure. The data obtained support the conclusion that the LMFBR conditions inhibit rapid sodium vaporization, and provide information on fuel fragmentation resulting from contact of hot fuel with liquid sodium.

TABLE V. Result of S-series Piston Autoclave Meltdown Tests

	S-3	S-4	S-5	S-6	S-7	S-8
Number of fueled pins	5	5	5	7	7	7
Mass UO_2, g	205	205	205	286	204	205
Ratio of sodium-to-fuel-pin areas	2.3	2.3	2.3	0.94	0.97	0.97
Initial sodium temperature, °F (°C)	338 (170)	329 (165)	329 (165)	410 (210)	932 (500)	932 (500)
Reactor period, ms	53	34	46	38	40	27
Maximum (local) fuel energy at first pressure pulse, J/g UO_2	2073	2245	2036	1973	1894	1852
Amplitude of largest pressure pulse, including delayed interactions, atm (MPa)	37 (3.7)	122 (12.2)	200 (20)	140 (14)	24 (2.4)	53 (5.3)
Calculated conversion from nuclear to mechanical energy based on energy at initial failure	2.1×10^{-5}	2.5×10^{-4}	1.9×10^{-3}	1.5×10^{-3}	6×10^{-6}	1.3×10^{-5}
Mass mean residue diameter, μm	2700	1240	220	400	300	1200[a]

[a]Only 26 g.

REFERENCES

1. E. W. Barts, L. W. Deitrich, J. G. Eberhart, A. K. Fischer, and C. C. Meek, *Summary and Evaluation--Fuel Dynamics Loss-of-flow Experiments (Tests L2, L3, and L4)*, ANL-75-57 (Sept 1975).

2. L. W. Deitrich, R. C. Doerner, T. H. Hughes, and A. E. Wright, *Summary and Evaluation of Fuel Dynamics Transient Overpower Experiments*, ANL-77-44 (June 1977).

3. M. A. Grolmes, R. E. Holtz, B. W. Spencer, C. E. Miller, and N. A. Kramer, "R-Series Loss-of-Flow Safety Experiments in TREAT," *Proc. Fast Reactor Safety Topical Meeting, Beverly Hills, Calif., April 2-4, 1974.* American Nuclear Soc. Hinsdale, Ill.

4. G. E. Culley, J. H. Scott, and J. E. Hanson, *Transient Overpower Response of Mixed Oxide Fuel Pins*, Trans. Am. Nucl. Soc. *15*(1), 341 (1972).

5. J. H. Scott, G. E. Culley, C. W. Hunter, and J. E. Hanson, "Microstructural Dependence of Failure in Mixed-Oxide LMFBR Fuel Pins," *Proc. Fast Reactor Safety Topical Meeting, Beverly Hills, Calif., April 2-4, 1974.* American Nuclear Soc., Hinsdale, Ill.

6. L. W. Deitrich, A. De Volpi, B. A. Feay, W. F. Murphy, and L. J. Harrison, *A Loss-of-Flow Simulation with Fresh FFTF-Type Pins*, Trans. Am. Nucl. Soc. *16*(1), 182 (1973).

7. J. C. Carter, L. W. Deitrich, A. De Volpi, C. C. Meek, W. F. Murphy, and J. G. Eberhart, ed., *The L2 Loss-of-flow Experiment*, ANL report in preparation.

8. A. K. Fischer, *Partial and Total Vapor Pressure from Molten Stainless Steel in Contact with Hot Fuel*, Trans. Am. Nucl. Soc. *19*(1), 277 (1974).

9. B. W. Spencer, M. A. Grolmes, R. E. Holtz, and C. E. Miller, *Cladding Motion and Blockages in R-Series Safety Experiments*, Trans. Am. Nucl. Soc. *19*(1), 238 (1974).

10. J. J. M. Snepvangers, H. H. Boswinkel, N. Vander Kely, H. Kwast, A. van der Linde, J. R. D. Stoute, and J. F. van de Vate, "Experimental Work on Fast Reactor Safety," *Proc. 4th UN Int. Conf. Peaceful Uses Atomic Energy*, Geneva, Paper 027 (1971).

11. H. Kwast, "The Behavior of Fast Reactor Fuel Pins Under Loss-of-Coolant Flow Conditions," *Proc. Fast Reactor Safety Topical Meeting, Beverly Hills, Calif., April 2-4, 1974.* American Nuclear Soc., Hinsdale, Ill.

12. H. Kwast, private communications (Mar 1974).

13. J. H. Cook, C. E. Holson, R. Villarreal, and J. F. Farr, *Plutonium Contamination Monitoring in the HFEF Hot Cells During the Sectioning of RAS-TREAT Mark-IIA Sodium Loops*, ANL/HFEF-006 (May 1975).

14. E. W. Barts, L. W. Deitrich, A. De Volpi, J. G. Eberhart, A. K. Fischer, P. H. Froehle, W. F. Murphy, D. Stahl, R. R. Stewart, J. P. Tylka, and L. J. Harrison, *Loss-of-Flow Simulations with Pre-Irradiated FFTF-Type Fuel Pins (Tests L3 and L4)*, Trans. Am. Nucl. Soc. *17*(1), 363 (1973).

15. A. K. Fischer, R. K. Lo, and E. W. Barts, *Fuel Dynamics Loss-of-flow Test L3 (Final Report)*, ANL-76-79 (June 1976).

16. J. G. Eberhart, R. K. Lo, and E. W. Barts, *Final Report on Test L4, A Loss-of-flow Experiment,* ANL-76-130 (Dec 1976).

17. C. E. Dickerman, L. E. Robinson, J. F. Boland, R. T. Purviance, and K. J. Schmidt, *First TREAT Experiment on High-Energy Fuel Failure of an Unirradiated Oxide Fast Reactor Fuel Pin in Flowing Sodium,* Trans. Am. Nucl. Soc. *12*(2), 370 (1969).

18. C. E. Dickerman, L. E. Robinson, A. K. Agrawal, W. F. Murphy, and A. E. Wright, *Initial TREAT Loop Experiments on LMFBR Oxide Fuel Behavior during a Power Excursion (Tests E1 and E2),* ANL-8099 (May 1974).

19. L. W. Deitrich, *Evaluation of Energy Conversion in TREAT Mark-II Loop Experiments,* Trans. Am. Nucl. Soc. *14*(2), 278 (1971).

20. S. M. Zivi, R. W. Wright, M. Epstein, F. J. Testa, G. Golfus, R. W. Mouring, J. J. Barghusen, and D. H. Cho, *Autoclave Tests S-11 and S-12 on Fuel-Coolant Interactions under Simulated Conditions of Prompt-Burst Disassembly,* Trans. Am. Nucl. Soc. *17*(1), 349 (1973).

21. R. W. Wright, J. J. Barghusen, S. M. Zivi, M. Epstein, R. O. Ivins, and R. W. Mouring, "Summary of Autoclave TREAT tests on Molten-Fuel-Coolant Interactions," *Proc. Fast Reactor Safety Topical Meeting, Beverly Hills, Calif., April 2-4, 1974.* American Nuclear Soc., Hinsdale, Ill.

22. H. A. Morewitz, D. Logan, and L. M. Haba, *Exploding Fuel Pin Experiments,* Trans. Am. Nucl. Soc. *14*(1), 279 (1971).

23. A. B. Rothman, A. K. Agrawal, R. T. Purviance, K. J. Schmidt, J. F. Boland, and R. D. Leggett, *Failure Threshold TREAT Experiment with an Unirradiated Prototypical FFTF Fuel Element,* Trans. Am. Nucl. Soc. *13*(2), 652 (1970).

24. R. C. Doerner, A. B. Rothman, A. De Volpi, C. E. Dickerman, L. W. Deitrich, D. Stahl, and W. F. Murphy, *Final Summary Report of Fuel-Dynamics Tests H2 and E4,* ANL-76-16 (Feb 1976).

25. R. C. Doerner, C. E. Dickerman, J. F. Boland, A. K. Agrawal, E. Maslowicz, R. T. Purviance, and J. E. Hanson, *Beyond Failure Transient Test of a Typical FFTF Fuel Element,* Trans. Am. Nucl. Soc. *14*(1), 279 (1971).

26. L. W. Deitrich, F. L. Willis, R. T. Purviance, K. J. Schmidt, C. E. Dickerman, and J. F. Boland, *High Energy Transient Meltdown of Irradiated UO_2 in a TREAT Mark-II Loop,* Trans. Am. Nucl. Soc. *13*(2), 652 (1970).

27. R. C. Doerner, C. E. Dickerman, A. B. Rothman, and M. E. Stephenson, *Irradiated Fuel Failure Experiment in a Fast Reactor Reactivity Accident (Test E6),* Trans. Am. Nucl. Soc. *17*(1), 284 (1973).

28. W. F. Murphy and D. H. Stahl, private communication (Apr 1975).

29. R. C. Doerner and A. De Volpi, *A Failure Experiment on High Power FFTF-Type Fuel in a Transient Overpower Accident (Test E7),* Trans. Am. Nucl. Soc. *18*(2), 212 (1974).

30. R. C. Doerner, W. F. Murphy, G. S. Stanford, and P. H. Froehle, *Final Summary Report of Fuel Dynamics Test E7,* ANL topical report in preparation.

31. A. E. Wright, L. W. Deitrich, W. F. Murphy, and A. De Volpi, *Transient Overpower Test H4 on FFTF-Type High-Power-Irradiated Fuel,* Trans. Am. Nucl. Soc. *19*(1), 259 (1974); also ANL topical report to be published.

32. A. E. Wright, A. B. Rothman, D. H. Stahl, A. De Volpi, T. H. Hughes, A. K. Agrawal, and L. J. Harrison, *In-Pile Failure Threshold Experiment (H5) with Pre-irradiated FFTF-Type Fuel*, Trans. Am. Nucl. Soc. *17*(2) (1974).

33. A. E. Wright, D. Stahl, G. S. Stanford, A. B. Rothman, C. E. Dickerman, and L. J. Harrison, *Transient Overpower Test H5 on FFTF-type Intermediate-power Fuel*, ANL topical report to be published.

34. T. Hikido and J. H. Field, *Molten Fuel Movement in Transient Overpower Tests of Irradiated Oxide Fuel*, GEAP-13549 (1969).

Distribution for ANL-77-40

Internal:

J. A. Kyger
A. Amorosi
L. Burris
D. W. Cissel
S. A. Davis
B. R. T. Frost
D. C. Rardin
R. G. Staker
R. J. Teunis
C. E. Till
R. S. Zeno
H. O. Monson
R. Avery
J. F. Marchaterre
A. J. Goldman
H. K. Fauske
B. D. LaMar
D. Rose
C. E. Dickerman (25)
L. W. Deitrich
D. R. Ferguson
R. A. Noland
S. H. Fistedis
L. Baker
R. H. Sevy
P. A. Lottes
D. H. Lennox
M. J. McDaniel
J. B. Heineman
M. Damakowski (5)
B. A. Korelc (4)
T. C. Chawla
T. H. Bauer
R. O. Brittan
D. J. Dever
A. De Volpi
R. C. Doerner
C. L. Fink
P. H. Froehle
A. E. Klickman
N. J. Koopman
R. K. Lo
R. O. McNary
R. J. Page
R. G. Palm
J. P. Regis
E. A. Rhodes
A. B. Rothman
L. A. Semenza
R. Simms
G. S. Stanford
R. R. Stewart
J. P. Tylka
A. E. Wright
I. Bornstein
R. E. Henry
A. B. Krisciunas
ANL Contract Copy
ANL Libraries (5)
TIS Files (6)

External:

ERDA-TIC, for distribution per UC-79p (282)
Manager, ERDA-CH
Chief, Chicago Patent Group
Director, ERDA-RDD (2)
Director, Reactor Programs Div., ERDA-CH
Director, CH-INEL
President, Argonne Universities Association
Reactor Analysis and Safety Division Review Committee:
W. Kerr, U. Michigan
M. Levenson, Electric Power Research Inst.
S. Levy, General Electric Co., San Jose
R. B. Nicholson, Exxon Nuclear Co., Inc.
D. Okrent, U. California, Los Angeles